Low-noise picosecond soliton transmission by use of concatenated nonlinear amplifying loop mirrors

Ildar Gabitov

L. D. Landau Institute for Theoretical Physics, Kosigina 2, 117940 Moscow, Russia

Darryl D. Holm and Benjamin P. Luce

Center for Nonlinear Studies and Theoretical Division, Los Alamos National Laboratory, Los Alamos, New Mexico 87545

Received April 8, 1996; revised manuscript received June 14, 1996

We compare two systems that are specially configured with loop mirrors to provide stable picosecond soliton transmission. One configuration, created by Smith and Doran [J. Opt. Soc. Am. B **12**, 1117 (1995)], uses nonlinear optical loop mirrors. This configuration is compared with another that uses nonlinear amplifying loop mirrors, the configuration of which we systematically determine from the amplitude and the pulse-width switching characteristics of the nonlinear optical loop mirror. It is found that the nonlinear optical loop mirror configuration allows stable pulse transmission with much less dispersive background waves than does the nonlinear optical loop mirror configuration. This clean performance is obtained at the cost of slightly lessening the parameter region of global stability of pulses. A technique for accurately estimating the region of global stability for amplitude and pulse-width perturbations of the stable pulse is also given. © 1997 Optical Society of America [S0740-3224(97)02804-X]

Nonlinear amplifying loop mirrors (NALM's) and nonlinear optical loop mirrors (NOLM's) are two all-optical devices that exploit the optical Kerr effect to switch the parameters of optical pulses.[1–3] For small input amplitudes or short loop lengths it can be shown that NALM's approximately cube the amplitude of pulses, leaving the phase unchanged.[4] It was shown[4,5] that this cubing effect can almost perfectly restore the soliton shape of solitons that have been distorted by losses. However, working in this cubing regime is unstable unless additional means are undertaken to stabilize pulses.

Recently, Smith and Doran[6] (SD) suggested that NOLM's operating past the first energy-switching peak could be effectively used as saturable absorbers to stabilize pulses in high-bit-rate (picosecond) transmission systems employing dispersion-shifted fiber [D = 1 ps/(nm km)]. SD have shown that stable picosecond pulse transmission over long distances is theoretically achievable if long segments of fiber followed by properly configured NOLM's with preamplification are concatenated, provided that some problems with pulse interactions that are due to strong dispersive background waves are overcome. In this paper we explore some of the advantages and disadvantages of substituting NALM's for NOLM's in this scheme. We closely compare a typical system configuration employing NALM's to a typical system configuration employing NOLM's that is taken from the SD paper. We find that the use of NALM's greatly reduces noise and pulse interactions at the cost of a slight decrease in the parameter region of global stability of the pulses.

To simulate these systems, we numerically integrate the damped nonlinear Schrödinger equation,

$$\frac{\partial q}{\partial Z} = -\gamma q + \frac{i}{2}\frac{\partial^2 q}{\partial T^2} + i|q|^2 q, \tag{1}$$

which describes the evolution of fiber optical pulses in standard soliton units, where q is the complex envelope of the electric field, Z is the fiber coordinate, γ is the damping coefficient, and T is the retarded time. SD have argued that using loop mirrors as saturable absorbers will be most applicable in picosecond soliton systems using dispersion-shifted fiber.[6] We henceforth assume that the optical fiber from which the entire system is constructed (including the loop mirrors) is dispersion-shifted fiber with D = 1 ps/(nm km) and with losses of 0.2 dB/km. We nondimensionalize to the time scale t_0 = (1/1.76) ps and a dispersion length (determined from D and t_0) of z_d = 0.2533 km. Therefore pulses with amplitude of the form $|q| = \eta\ \mathrm{sech}(\beta T)$ will have a FWHM intensity pulse width of $(1/\beta)$ ps. At these scales we have γ = 0.0058, and nondimensional distances are given by $\Delta Z = \Delta z/z_d$, where Δz is the distance in kilometers.

The schematic of a generalized loop mirror (GLM) that includes both NALM's and NOLM's as special cases is drawn in Fig. 1. At the input, optical pulses are preamplified linearly with gain G_{pre}. The pulses are then split by the coupler with power-splitting ratio α into counterpropagating pulses in a loop of length L. The clockwise-propagating pulse is immediately amplified with gain G. The other pulse is also eventually amplified with gain G

0740-3224/97/0701850-06$10.00

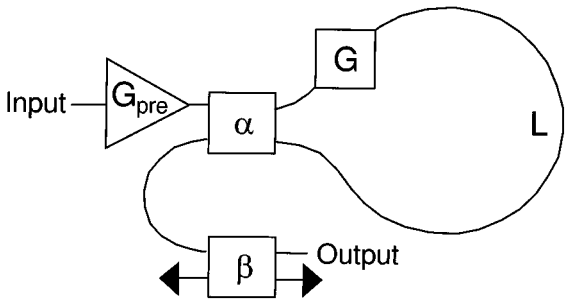

Fig. 1. Generalized loop mirror.

after propagating around the loop. The output pulse then passes through an additional coupler with splitting ratio β. The reason for the additional coupler will become apparent. We assume that any pulse component reflected back up the input is absorbed by optical isolaters not shown in the schematic. We also assume lossless couplers, splices, etc., although such losses, if known, may be taken into account for system designs of the type we discuss.

The GLM reduces to a NOLM (plus preamplifier and additional coupler) if we impose $\alpha \neq 0.5$ and $G = 0$ dB (no amplifier in the loop) and to a NALM (plus preamplifier and additional coupler) if we impose $\alpha = 0.5$ and $G > 0$ dB.

By way of example, we now review the switching properties of the NOLM and its application by SD. The NOLM configuration of the GLM that we shall discuss is $G_{\text{pre}} = 4$ dB, $\alpha = 0.1$, $G = 0$ dB, $L = 1.5$ km, and $\beta = 1$ (that is, no additional coupler). This configuration is specified in Fig. 12 of the SD paper,[6] and it is typical of the systems discussed in this paper. This figure shows undesirable pulse interactions occurring between widely separated pulses when 15-km segments of optical fiber followed by the NOLM are concatenated (same fiber type as used here). We call this configuration the SD example for the remainder of this paper.

SD also allowed filtering (restricted bandwidth) in the preamplifier. They found that strong-enough filtering could significantly reduce the self-frequency shift (Raman effect). We do not find it necessary to discuss filtering for the purposes of this paper, partially because this point was adequately addressed by SD, and partially to give a cleaner comparison of systems that use NOLM's and NALM's. However, we confirmed that properly applied filtering, especially at the input of the loop mirrors, seems to improve the performance of all the systems described here in the same way as described by SD. Filtering also seems to help stabilize these systems with respect to other higher-order effects, such as third-order dispersion, although these effects probably impose subtle limits on the bit rates of these systems. A full study of these effects remains to be done, with the best approach now probably being some experimental tests.

We now discuss the energetics of the fiber–NOLM system, which provides much fundamental information. The nondimensional energy of pulses $q(T)$ is given by

$$E = \int_{-\infty}^{+\infty} |q(T)|^2 \mathrm{d}T.$$

For example, for pulses with amplitude $|q(T)| = \eta\ \mathrm{sech}(\beta T)$, we have

$$E = 2\eta^2/\beta. \tag{2}$$

Because of the smallness of the damping parameter γ, soliton pulses with the initial form $q_0 = \eta\ \mathrm{sech}(\eta T)$ launched into a fiber segment will decay adiabatically; that is, they will retain their soliton form, with amplitude given by

$$|q(Z)| = \eta \exp(-2\gamma Z)\mathrm{sech}[\eta \exp(-2\gamma Z)T].$$

It follows that the energy of the pulse is given by

$$E(Z) = E(0)\exp(-2\gamma Z),$$

where $E(0) = 2\eta$.

The function $f(\ )$ describing the energy transformation generated by the NOLM for soliton input is called the energy-switching function (ESF). Because of the adiabatic nature of the propagation stage, the system ESF for a system element consisting of a single fiber segment of length ΔZ followed by the NOLM–GLM, for soliton input, is given by

$$E_{\text{out}} = f[\exp(-2\gamma \Delta Z)E_{\text{in}}].$$

The system ESF for the SD example (without filtering) is plotted in Fig. 2. Also shown on the plot are amplitude and pulse-width parameters for sech fits to the input and the output pulses of the NOLM (these parameters are discussed below). This curve was generated by the adiabatic approximation for propagation in the 15-km segment, followed by a full numerical simulation, including losses, of pulses in the NOLM. The idea of SD can be understood most simply by assuming (for the moment) that the output of the NOLM is always a perfect soliton with energy determined by the NOLM ESF. In this case the fate of an input pulse after repeated propagation through 15-km segments followed by NOLM's can be found by iterating the total ESF. As can be seen from inspecting the system, initial energies greater than the critical threshold of 1.6 and less than 3.2 will eventually converge

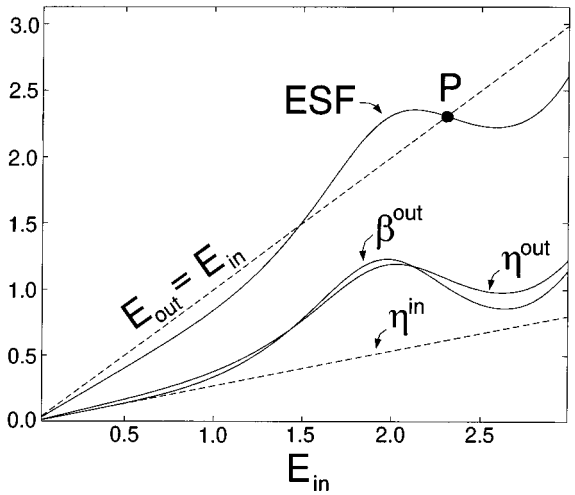

Fig. 2. ESF for the NOLM–GLM in the SD example with $G_{\text{pre}} = 4$ dB, $\alpha = 0.1$, $G = 0$ dB, $L = 1.5$ km, and $\beta = 1$.

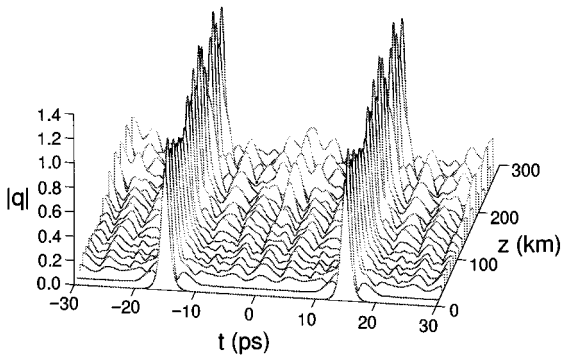

Fig. 3. Simulation of the SD example without filtering. Substantial background waves are seen to be generated from the pulses.

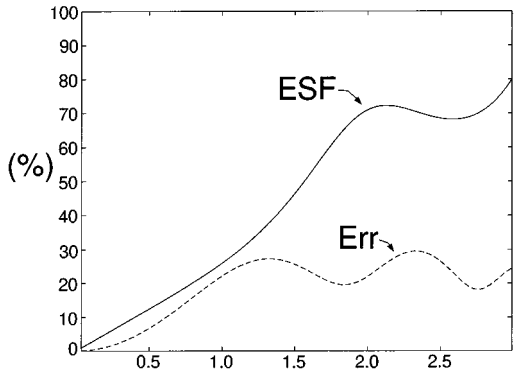

Fig. 4. Least-squares percentage error Err in the output pulse of the NOLM with soliton input for the SD example discussed in the text.

on the fixed point marked P in Fig. 2. The wide basin of attraction of the fixed point is due to careful configuration of the system by SD.

In reality, the output of the NOLM always contains some dispersive background waves, and therefore the fixed point of the system ESF is not enough to guarantee the existence of a stable pulse. Fortunately, a relatively stable pulse does emerge in simulations, as was reported by SD. A plot of our own simulation of the SD example for two pulses (and without filtering) appears in Fig. 3. The figure shows strong dispersive background waves generated along with the stable pulses (we have plotted $|q|$ instead of the usual practice of plotting the energy density $|q|^2$ to make these waves readily apparent). These dispersive waves correspond to large sidelobes in the frequency spectrum of the pulse. We remark that these background waves are really intrinsic to this system configuration—they are generated by the action of the NOLM on the pulses and are only slightly lessened by filtering.

SD found strong interactions between very widely separated pulses in the SD example described above and in similar system configurations employing NOLM's (see Figs. 11 and 12 of their paper), which they suggest are due to the dispersive background waves. They observed that these interactions are highly sensitive to system parameters. We remark that these interactions are also sensitive to numerical simulation parameters, such as number of Fourier modes or integration technique, and therefore that little can yet be confidently asserted about the details of these interactions. In spite of these uncertainties, the robustness of the dispersive waves in simulations suggests that strong dispersive background waves will occur in real systems and are very likely to cause strong interactions between pulses. It is therefore of utmost importance to minimize these waves.

We now examine in greater detail how loop mirrors and the systems that employ them switch primary pulse parameters such as amplitude and pulse width as well as energy. Such information will be useful if, for soliton input, the output pulse can be closely approximated by a sech function. We assume now the form $q_{\mathrm{in}} = \eta^{\mathrm{in}}\,\mathrm{sech}(\eta^{\mathrm{in}}T)$ for the input pulse, which has energy $E_{\mathrm{in}} = 2\eta^{\mathrm{in}}$. For a numerically calculated output pulse q_{out} we first measure the peak amplitude η^{out} and energy E_{out} of the pulse and then compute its least-squares difference from a pulse of the form $q_{\mathrm{fit}} = \exp(i\phi)\eta^{\mathrm{out}}\,\mathrm{sech}(\beta^{\mathrm{out}}T)$ having the same phase (ϕ) at the peak amplitude and the same energy [so that $\beta^{\mathrm{out}} = 2(\eta^{\mathrm{out}})^2/E_{\mathrm{out}}$]. We define the percentage error of the output pulse with respect to q_{fit} to be

$$\mathrm{Err} = \frac{100}{\sqrt{E_{\mathrm{out}}}}\sqrt{\int_{-\infty}^{+\infty}|q_{\mathrm{out}} - q_{\mathrm{fit}}|^2\,\mathrm{d}T}.$$

Note that this error measurement is sensitive to changes in phase across the pulse and to amplitude deviations from the sech shape. In the following we will measure the error and the switched-pulse parameters E_{out}, η^{out}, and β^{out} as functions of $E_{\mathrm{in}}(\eta^{\mathrm{in}})$ for loop mirrors by themselves and for the entire system's elements consisting of long fiber segments followed by loop mirrors. We configure an element first by measuring the loop mirror switching characteristics and then by attempting to create a stable fixed point of the system element by use of the switching information.

For the SD example the error Err for the system element consisting of the 15-km segment followed by the NOLM is plotted in Fig. 4 along with the (arbitrarily normalized) ESF of the element. The switched-pulse parameters are plotted in Fig. 2 (in this plot, the parameter η^{in} is the input amplitude at the NOLM, not the element input amplitude $E_{\mathrm{in}}/2$). We can see from Fig. 4 that the error at the fixed point P is $\sim 30\%$. Characterization of the output pulse by only amplitude and pulse width is somewhat dubious in this case since the pulse contains nonsech features that can contribute significantly to the background radiation. Nevertheless, it is seen from Fig. 2 that the switched parameters η^{out} and β^{out} are approximately equal at the fixed-point input energy, meaning that the output pulse has the proper balance between amplitude and pulse width of a soliton. Also, the numerical value of β^{out} is greater than η^{in} at the fixed point, so the NOLM is providing some necessary pulse compression. The propagation distance to decrease the output pulses amplitude from η^{out} and β^{out} to the value of η^{in} at the fixed point is approximately correct (this actually follows from the existence of the fixed point P in the ESF). The

NOLM–GLM system is thus nearly optimized to support a stable solitonlike fixed point, which is realized in simulations.

We now consider a NALM–GLM configuration with $G_{\text{pre}} = 0$ dB, $\alpha = 0.5$, $G = 6$ dB, $L = 1.5$ km, and with $\beta = 1$ (no additional coupler for the moment). The parameter L has been chosen to match the SD example. The gain G has been chosen small enough that the ESF of the NALM is not too narrowly peaked at the first switching peak to maximize stability. However, G is large enough to produce an output amplitude near the switching peak that is greater than the pulse width. The latter consideration allows the use of the additional coupler to equalize amplitude and pulse width, instead of an additional amplifier.

Figure 5 shows the output pulse error along with the (arbitrarily normalized) NALM–ESF. In this case the error just past the switching peak is seen to be ~15%, so characterization of the output pulse with the sech fit is more justified in this case than for the SD example. In particular, the error has a local minimum just beyond the switching peak, which we find to be a general characteristic of NALM's. In contrast, NOLM's usually have a local maximum in error just beyond the switching peak. Therefore it seems wise to attempt to establish a fixed point slightly past the switching peak of the NALM. Also note that, owing to the pulse cubing effects of NALM's at low energies, the ESF of the NALM rises quintically from zero at low amplitudes (the ESF's of NOLM's always rise linearly at low energies; see Fig. 2). This extremely gradual increase from zero, which occurs for all low-energy inputs, is very effective for suppressing background waves, and is really one of the greatest motivations for attempting to use concatenated NALM's for producing stable pulses.

We now discuss the stability of fixed points with the NALM. The NALM–ESF given in Fig. 5 has a very low local minimum (a large extinction ratio) located at $E_{\text{in}} \cong 1.7$. To provide maximal linear and global stability to the stable fixed point, SD used a small coupler-splitting ratio specifically to avoid this feature in the NOLM (also see Fig. 2).[6] If the extinction ratio is sufficiently small,

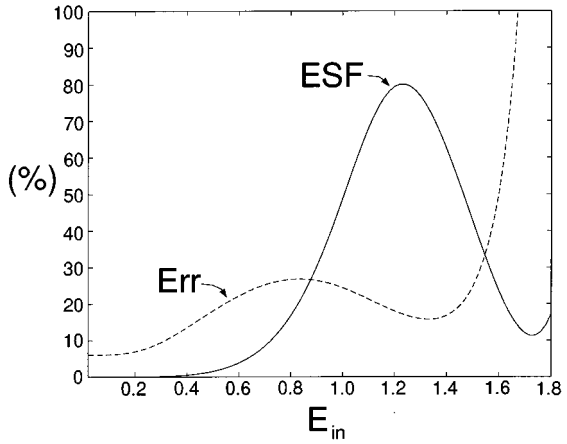

Fig. 5. Least-squares percentage error Err in the output pulse of the NALM with soliton input for the configuration discussed in the text.

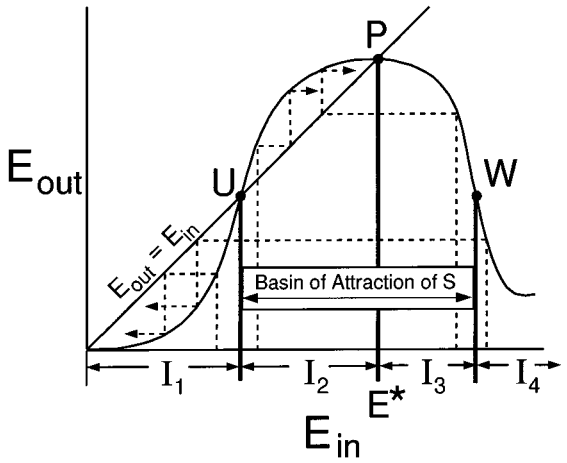

Fig. 6. Illustration of the iterated system ESF, showing the basin of attraction of the fixed point P, and the iterations of points from four different intervals.

there is substantial freedom in how far past the switching peak the fixed point may be placed (subject to other constraints, such as matching output amplitudes and pulse widths). However, most NALM configurations have large extinction ratios. Thus, to obtain maximal stability for the NALM case, one must place the fixed point only slightly past the switching peaks to center the basin of attraction of the fixed point around the fixed point. The basin structure is illustrated schematically in Fig. 6. Fortunately, such a choice meshes nicely with the minimum in pulse-quality error just past the switching peak and also provides strong linear stability for the fixed point because the slope of the ESF near the switching peak is small. It is obvious from these considerations that the parameter region of global stability of a NALM fixed point will be more limited than that of a NOLM. This tends to widen the basin of attraction by decreasing the sharpness of the switching peak. The success of this technique will therefore depend on whether this limitation is too stringent in real systems. Maximal stability with NALM's is also best achieved by keeping the gain of the NALM somewhat low. This tends to decrease the sharpness of the switching peak, which clearly widens the basin of attraction for the stable pulse.

The fact that the output pulse is quite sechlike at our target fixed point now justifies an attempt to calculate a system configuration with a stable fixed point by use of the switched parameters η^{in}, η^{out}, and β^{out}, which are plotted in Fig. 7 along with the NALM–ESF (not the total ESF, because we have not yet determined a propagation distance preceding the NALM). We choose to try to create a fixed point at $E_{\text{in}} = 1.28 (\eta^{\text{in}} = 0.64)$.

First, based on the values of $\eta^{\text{out}} = 1.2607$ and $\beta^{\text{out}} = 0.8438$, which occur at $E_{\text{in}} = 1.28$, we calculate that the additional coupler-splitting ratio β needs to be ~0.45 to make the amplitude and the pulse width match (recall that such an adjustment was not needed in the SD example because η^{out} and β^{out} were equal at the fixed point). We henceforth denote the output amplitude as $\eta^p = \beta^{\text{out}} = 0.8438$.

Next we must choose the propagation distance such

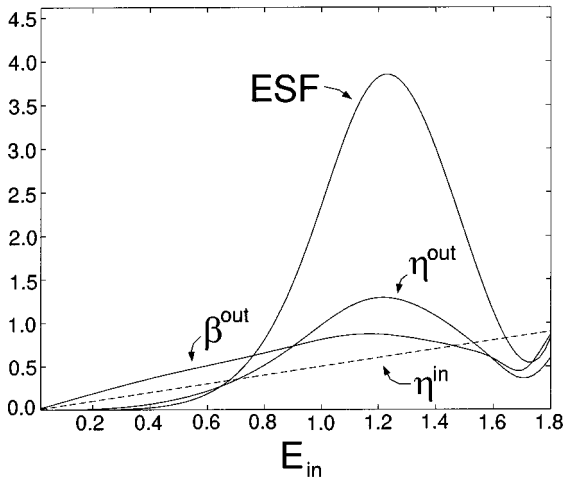

Fig. 7. ESF and parameter-switching curves of the NALM for the configuration given in the text.

that a soliton launched with amplitude η^p will decay to a soliton of amplitude $\eta^{\text{in}} = 0.64$. Since $\gamma = 0.0058$, we have

$$\Delta Z = \frac{1}{2} \log \frac{\eta^p}{\eta^{\text{in}}} = 23.7,$$

which corresponds almost exactly to 6 km. If this distance seems short, recall that the dispersion distances of the pulses that we are considering are each ~0.25 km!

On the other hand, although the loop designs are comparable, the reader may feel that our comparison of this system to the SD example, which has a 15-km spacing, is unfair. In other words, perhaps the comparison should be between the best possible designs using NOLM's with those using NALM's over the same propagation distance instead of with similar loop parameters. It turns out that the comparisons made either way yield similar results and that the stability of the NALM designs depend more on the loop parameters than on the propagation distance. For example, if one considers a NALM–GLM configuration with $G_{\text{pre}} = 0$ dB, $\alpha = 0.5$, $G = 7$ dB, $L = 0.6$ km, and with $\beta = 0.5$ (an additional 3-dB coupler on output), then this configuration, by means of the procedure carried out above, results in a stable pulse at a propagation distance of ~14 km. The stability of this pulse is just slightly weaker than in the 6-km NALM example because the gain in the loop mirror is slightly higher (the reason for this is made clear below).

With the parameters derived above, the ESF of the complete 6-km system element appears as plotted in Fig. 8, which also shows the parameter-switching curves for the element. The fixed point P in the ESF can be seen, as well as the equality of the output amplitude and pulse-width parameters at the fixed-point energy.

When the concatenated system is simulated with these parameters with an initial pulse of the form $q_0 = \eta^p \operatorname{sech}(\eta^p T)$, a stable pulse does indeed emerge that is very close to the initial condition. A simulation of two such pulses separated at 20-ps spacing is shown in Fig. 9. The adiabatic assumption for the propagation stage was not used here. Note that the amplitude is extremely smooth overall with no apparent dispersive background and no apparent interactions between the pulses (compare with Fig. 3). We emphasize that filtering has not been used in this simulation to diminish noise or interactions; the noise suppression is coming from the pulse-cubing effect of the NALM at low energies, and may also be partially due to the superior sech fit to the output pulse of the NALM for soliton input. The spectra of the pulses (which we have not shown) is smooth and closely resembles that of the initial soliton pulses. The phase profiles of the stable pulses are also fairly flat.

As can be seen from Fig. 9, the stable pulses are actually slightly broader at their bases than the initial solitons. This can cause strong interactions similar to those described by SD if the pulses are spaced too closely. Based on our simulations, we recommend that pulses with pulse width τ_s immediately after the NALM should be separated by $\sim 20\tau_s$ to safely avoid strong interactions. This spacing limit allows for pulses that roughly double their pulse width between each pair of NALM's before reaching a minimum spacing of ten pulse widths.

We now examine the global stability of the stable pulses in more detail. Observe from Fig. 6 that the intervals marked I_2 and I_3 make up the relevant part of the basin of attraction of the fixed point P. We now hypoth-

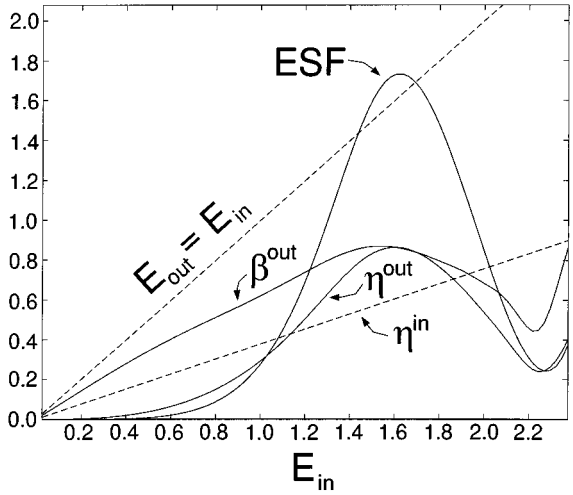

Fig. 8. Complete system ESF and parameter-switching curves of the configuration with the NALM described in the text.

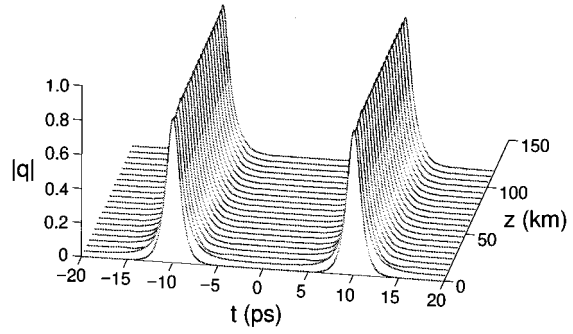

Fig. 9. Simulation of the system configuration with a NALM discussed in the text. It is seen that the NALM succeeds nicely in suppressing background waves.

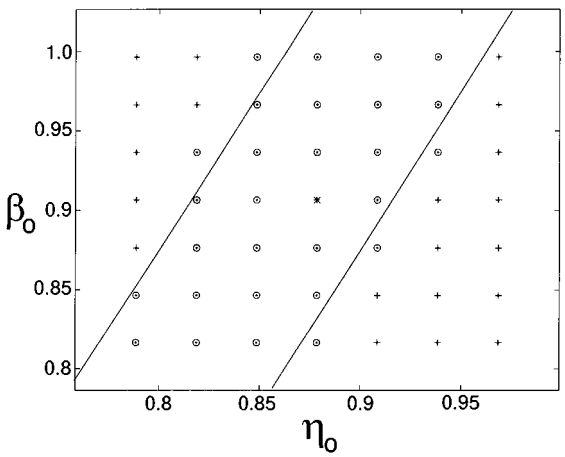

Fig. 10. Global stability chart for the stable pulse under amplitude and pulse-width perturbations for the system configuration with a NALM. The circles indicate initial pulses that relaxed to the stable pulse, and the plus signs indicate initial pulses that relaxed to zero. The asterisk locates the fixed point, which lies close to the point $(\eta^p, \eta^p) = (0.875, 0.91)$.

esize that these intervals roughly determine the maximum perturbations in energy that the stable pulse can withstand and still regain its initial pulse width. We investigate this hypothesis for amplitude and pulse-width perturbations. Assuming a perturbed stable pulse of approximately the form

$$q_0 = (\eta^p + \delta\eta)\mathrm{sech}[(\eta^p + \delta\beta)T], \tag{3}$$

the first variation of the energy of this pulse from the stable pulse is

$$\delta E = 4\delta\eta - 2\delta\beta.$$

If we let δE equal the lengths of I_2 and I_3 separately, which for $G = 6$ dB are both ~ 0.35, and solve for $\delta\beta$ in terms of $\delta\eta$, the hypothesis predicts two straight line stability boundaries in the (η, β) plane of slope 2 that pass through the points $(\eta^p \pm \delta E/4, \eta^p)$, respectively.

To check this hypothesis, we simulated directly the evolutions of perturbations in amplitude and pulse width of the numerically found stable pulse. Figure 10 shows the results of the experiment for a grid of initial amplitudes and pulse widths. The circles indicate the initial amplitudes and pulse widths that relaxed to the stable pulse, and the plus signs represent initial pulses that died away. Also shown on the plot are the stability boundaries predicted above. It can be seen that they agree fairly well with the numerical results.

In conclusion, we have compared the uses of NOLM's and NALM's as saturable absorbers to stabilize pulses in picosecond transmission systems. The NALM's are found to be vastly superior for suppressing background dispersive waves and therefore pulse interactions. However, the NALM technique results in smaller global stability regions for the stable pulses. We also found that the global stability region for amplitude and pulse-width perturbations could be accurately predicted by relating the first variation of the pulse energy to the NALM ESF.

ACKNOWLEDGMENTS

We thank Mac Hyman and William L. Kath for useful discussions. This work was performed under U.S. Department of Energy contract W-7405-ENG-36 and U.S. Department of Energy Program in Applied Mathematical Sciences contract KC-07-01-01.

REFERENCES

1. M. E. Fermann, F. Haberl, M. Hofer, and H. Hochreiter, "Nonlinear amplifying loop mirror," Opt. Lett. **15**, 752–754 (1990).
2. N. J. Doran and D. Wood, "Nonlinear-optical loop mirror," Opt. Lett. **13**, 56–58 (1988).
3. K. J. Blow, N. J. Doran, and B. K. Nayar, "Experimental demonstration of optical soliton switching in an all-fiber nonlinear Sagnac interferometer," Opt. Lett. **14**, 754–756 (1989).
4. M. Matsumoto, A. Hasegawa, and Y. Kodama, "Adiabatic amplification of solitons by means of nonlinear amplifying loop mirrors," Opt. Lett. **19**, 1019–1021 (1994).
5. I. Gabitov, D. Holm, B. P. Luce, and A. Mattheus, "Recovery of solitons with nonlinear amplifying loop mirrors," Opt. Lett. **20**, 2490–2492 (1995).
6. N. J. Smith and N. J. Doran, "Picosecond soliton transmission using concatenated nonlinear optical loop-mirror intensity filters," J. Opt. Soc. Am. B **12**, 1117–1125 (1995).